Philosophical Magazine
Publication details, including instructions for authors and subscription information:
http://www.tandfonline.com/loi/tphm20

Tunable interplay between superconductivity and correlations in nanoscopic heterostructures

T. Domański[a], J. Barański[a] & M. Zapalska[a]
[a] Institute of Physics, M. Curie-Skłodowska University, 20-031Lublin, Poland.
Published online: 07 Oct 2014.

Philosophical Magazine, 2014
http://dx.doi.org/10.1080/14786435.2014.965766

Taylor & Francis
Taylor & Francis Group

Tunable interplay between superconductivity and correlations in nanoscopic heterostructures

T. Domański*, J. Barański and M. Zapalska

Institute of Physics, M. Curie-Skłodowska University, 20-031 Lublin, Poland

(*Received 29 July 2014; accepted 11 September 2014*)

Artificial heterostructures consisting of the superconducting electrode(s) and the free electron reservoir(s) interconnected through various nanoscopic objects, like: quantum dots, nanowires or molecules enable a fully controllable confrontation of the correlation effects with electron pairing. Discrete energy spectrum of the nanoscopic objects (due to the quantum size effect) strongly depends on the many-body effects. Via the proximity effect, these nanoscopic objects are converted into the superconducting grains. Since the coupling to external electrodes can be varied experimentally, this enables a fully controllable investigation of an interplay between the electron correlations and superconductivity. In this work, we explore the subgap (Shiba) states arising from the induced pairing and analyse their influence on the Kondo-type correlations. This issue is currently widely explored using various nanoscopic devices.

Keywords: proximity effect; Shiba states; electron correlations; Kondo effect

1. Introduction

Recent experiments using the self-assembled quantum dots [1], semiconducting nanowires [2,3] and carbon nanotubes [4,5] embedded between one superconducting and another conducting electrode have provided a clear evidence for the Shiba (or Andreev) states formed in a subgap regime $|E| \leq \Delta$ (where Δ denotes the energy gap of superconductor). Such states originate solely from the on-dot pairing spread on the nanoscopic objects via the proximity effect. They have been practically observed in the low-bias tunneling conductance due to the anomalous Andreev scattering. Similar subgap states have also been reported for the quantum objects hybridized with both superconducting electrodes [6–8], where they effectively invert the sign of Josephson current, inducing $0 - \pi$ transition [9].

An important role of quantum impurities has been addressed earlier mainly by trying to check how they affect the superconducting bulk materials [10]. It has been established that non-magnetic impurities are rather inefficient for the isotropic superconductors [11] or have a weak detrimental influence on the anisotropic superconductors [12]. As far as the magnetic impurities are concerned, they proved to be more destructive for the superconducting host materials, because of the subgap Shiba states [13]. These in-gap states substantially reduce the energy gap of the superconducting hosts and suppress their critical temperature.

*Corresponding author. Email: doman@kft.umcs.lublin.pl

The present day studies using the nanoscopic heterojunctions are able to investigate a completely opposite influence, namely of the induced pairing on the electron correlations due the Coulomb repulsion. At sufficiently low temperatures, one can explore even the Kondo-type correlations, when the spin of quantum impurity is screened by spins of the mobile electrons forming the many-body singlet state [14]. Since superconductivity and antiferromagnetism represent the competing phenomena it is natural to suspect that the induced on-dot pairing should have a detrimental influence on the Kondo effect. Such competition can be explored in a tunable way because the hybridizations with external leads can be varied by few orders of magnitude. Additionally, by applying an external magnetic field B, one can change the superconductor gap $\Delta(B)$ [2]. Theoretical and experimental aspects of such tunable studies of the quantum dots connected to the superconducting leads are surveyed e.g. in the articles [3,15–17].

In this work, we comment on the origin of the subgap states both, in the uncorrelated and in the correlated quantum dot attached between the metallic and superconducting electrodes. Our analysis extends the previous study [18] of the quantum impurity coupled only to the superconducting reservoir. In Sections 5 and 6, we also consider how the proximity induced on-dot pairing affects the Kondo-type correlations.

2. Microscopic model

For description of a heterojunction in which the correlated quantum impurity is on one side attached to the metallic (N) and on other side to the superconducting (S) electrode we can use the Anderson impurity Hamiltonian

$$\hat{H} = \hat{H}_N + \hat{H}_S + \sum_{\sigma} \epsilon_d \hat{d}^{\dagger}_{\sigma}\hat{d}_{\sigma} + U_d\, \hat{n}_{d\uparrow}\hat{n}_{d\downarrow} + \sum_{\mathbf{k},\sigma,\beta} \left(V_{\mathbf{k}\beta}\, \hat{d}^{\dagger}_{\sigma}\hat{c}_{\mathbf{k}\sigma\beta} + V^{*}_{\mathbf{k}\beta}\hat{c}^{\dagger}_{\mathbf{k}\sigma\beta}\hat{d}_{\sigma} \right). \quad (1)$$

The external reservoirs of mobile electrons are assumed as the free fermion gas $\hat{H}_N = \sum_{\mathbf{k},\sigma} \xi_{\mathbf{k}N}\hat{c}^{\dagger}_{\mathbf{k}\sigma N}\hat{c}_{\mathbf{k}\sigma N}$ and as the BCS-type superconductor $\hat{H}_S = \sum_{\mathbf{k},\sigma} \xi_{\mathbf{k}S}\hat{c}^{\dagger}_{\mathbf{k}\sigma S}\hat{c}_{\mathbf{k}\sigma S} - \sum_{\mathbf{k}} \Delta \left(\hat{c}^{\dagger}_{\mathbf{k}\uparrow S}\hat{c}^{\dagger}_{-\mathbf{k}\downarrow S} + \hat{c}_{-\mathbf{k}\downarrow S}\hat{c}_{\mathbf{k}\uparrow S} \right)$. The corresponding electron energies $\xi_{\mathbf{k}\beta} = \varepsilon_{\mathbf{k}\beta} - \mu_\beta$ are measured with respect to the chemical potentials μ_β, which can be detuned by an external voltage V (leading to $\mu_N = \mu_S + eV$). As usually, the annihilation (creation) operators $\hat{d}^{(\dagger)}_{\sigma}$ refer to the quantum impurity and $\hat{c}^{(\dagger)}_{\mathbf{k}\sigma\beta}$ to mobile electrons with spin $\sigma = \uparrow, \downarrow$. Energy level of the quantum dot is denoted by ε_d. A combined effect of the repulsive Coulomb potential U_d (between opposite spin electrons) and the hybridization $V_{\mathbf{k}\beta}$ (between the localized and mobile electrons) is responsible for the many-body effects.

In what follows, we focus on the low-energy regime, safely narrower than the superconductor energy gap Δ. Under such conditions, we can use the wide-band limit approximation $|V_{\mathbf{k}\beta}| \ll D$ (where $-D/2 \leq \varepsilon_{\mathbf{k}\beta} \leq D/2$). We also impose the constant couplings $\Gamma_\beta = 2\pi \sum_{\mathbf{k},\beta} |V_{\mathbf{k}\beta}|^2 \delta(\omega - \xi_{\mathbf{k}\beta})$.

3. Proximity effect

Since the off-diagonal order leaks onto the quantum impurity, we have to introduce the single-particle Green's function $\boldsymbol{G}_d(\tau, \tau') = \langle\langle \hat{\Psi}_d(\tau);\, \hat{\Psi}^{\dagger}_d(\tau') \rangle\rangle$ in the Nambu spinor representation $\hat{\Psi}^{\dagger}_d = (\hat{d}^{\dagger}_{\uparrow}, \hat{d}_{\downarrow})$, $\hat{\Psi}_d = (\hat{\Psi}^{\dagger}_d)^{\dagger}$. Under equilibrium conditions the Green's function

$\boldsymbol{G}_d(\tau, \tau')$ depends only on time difference $\tau - \tau'$ and its Fourier transform can be expressed as

$$[\boldsymbol{G}_d(\omega)]^{-1} = \begin{pmatrix} \omega - \varepsilon_d & 0 \\ 0 & \omega + \varepsilon_d \end{pmatrix} - \boldsymbol{\Sigma}_d^0(\omega) - \boldsymbol{\Sigma}_d^U(\omega). \tag{2}$$

The first component $\boldsymbol{\Sigma}_d^0$ of the selfenergy describes the influence of the hybridization $V_{\mathbf{k}\beta}$ in the uncorrelated ($U_d = 0$) quantum impurity. This part is known exactly. Roughly speaking, it is responsible for: (a) a finite life-time of the quantum impurity states (broadening of the energy levels) and (b) the induced on-dot pairing. As far as the second contribution $\boldsymbol{\Sigma}_d^U$ is concerned it describes the correlation effects due to the Coulomb repulsion U_d between opposite-spin electrons.

The selfenergy $\boldsymbol{\Sigma}_d^0(\omega)$ can be expressed by the (exact) bubble diagram

$$\boldsymbol{\Sigma}_d^0(\omega) = \sum_{\mathbf{k},\beta} \left| V_{\mathbf{k}\beta} \right|^2 \boldsymbol{g}_\beta(\mathbf{k}, \omega), \tag{3}$$

where $\boldsymbol{g}_\beta(\mathbf{k}, \omega)$ denote the single-particle Green's functions of the external leads. The free fermion gas of the metallic (N) electrode is characterized by a diagonal propagator

$$\boldsymbol{g}_N(\mathbf{k}, \omega) = \begin{pmatrix} \frac{1}{\omega - \xi_{\mathbf{k}N}} & 0 \\ 0 & \frac{1}{\omega + \xi_{\mathbf{k}N}} \end{pmatrix} \tag{4}$$

and the BCS superconductor by a full matrix structure

$$\boldsymbol{g}_S(\mathbf{k}, \omega) = \begin{pmatrix} \frac{u_{\mathbf{k}}^2}{\omega - E_{\mathbf{k}}} + \frac{v_{\mathbf{k}}^2}{\omega + E_{\mathbf{k}}} & \frac{-u_{\mathbf{k}} v_{\mathbf{k}}}{\omega - E_{\mathbf{k}}} + \frac{u_{\mathbf{k}} v_{\mathbf{k}}}{\omega + E_{\mathbf{k}}} \\ \frac{-u_{\mathbf{k}} v_{\mathbf{k}}}{\omega - E_{\mathbf{k}}} + \frac{u_{\mathbf{k}} v_{\mathbf{k}}}{\omega + E_{\mathbf{k}}} & \frac{u_{\mathbf{k}}^2}{\omega + E_{\mathbf{k}}} + \frac{v_{\mathbf{k}}^2}{\omega - E_{\mathbf{k}}} \end{pmatrix}. \tag{5}$$

with $E_{\mathbf{k}} = \sqrt{\xi_{\mathbf{k}S}^2 + \Delta^2}$ and $u_{\mathbf{k}}^2, v_{\mathbf{k}}^2 = \frac{1}{2}\left[1 \pm \frac{\xi_{\mathbf{k}S}}{E_{\mathbf{k}}}\right]$, $u_{\mathbf{k}} v_{\mathbf{k}} = \frac{\Delta}{2E_{\mathbf{k}}}$. Neglecting the band edge effects (the wide-band limit approximation) one obtains the following explicit expression

$$\boldsymbol{\Sigma}_d^0(\omega) = -\frac{\Gamma_N}{2} \begin{pmatrix} i & 0 \\ 0 & i \end{pmatrix} - \frac{\Gamma_S}{2} \begin{pmatrix} 1 & \frac{\Delta}{\omega} \\ \frac{\Delta}{\omega} & 1 \end{pmatrix} \times \begin{cases} \frac{\omega}{\sqrt{\Delta^2 - \omega^2}} & \text{for } |\omega| < \Delta, \\ \frac{i\,|\omega|}{\sqrt{\omega^2 - \Delta^2}} & \text{for } |\omega| > \Delta. \end{cases} \tag{6}$$

To determine the second contribution $\Sigma_d^U(\omega)$, one has to rely on approximations for the correlation effects. Extensive studies of this issue have been done adopting various methods, in particular, decoupling for the equations of motion of Green's functions [19], slave boson technique [20,21], the generalized non-crossing approximation [22], the iterative perturbation method [23,24], dynamical mean field approximation [25], numerical renormalization group approach [26,27], modified equation of motion approach [28], functional renormalization group [29], cotunneling approach [30], Quantum Monte Carlo simulations [31] and other [32,33]. Some of the main correlation effects will be discussed in the Section 6.

4. Shiba states of the uncorrelated quantum dot

We first consider spectroscopic signatures of the induced on-dot pairing which appear due to Γ_S. Upon neglecting the correlation effects, the Green's function (2) can be expressed explicitly. In the subgap regime $|\omega| < \Delta$, we have

$$[\boldsymbol{G}_d(\omega)]^{-1} = \begin{pmatrix} \tilde{\omega} + \varepsilon_d + i\Gamma_N/2 & \tilde{\Gamma}_s/2 \\ \tilde{\Gamma}_s/2 & \tilde{\omega} - \varepsilon_d + i\Gamma_N/2 \end{pmatrix}, \tag{7}$$

where $\tilde{\omega} = \omega + \frac{\Gamma_S}{2}\frac{\omega}{\sqrt{\Delta^2-\omega^2}}$ and $\tilde{\Gamma}_s = \Gamma_S \frac{\Delta}{\sqrt{\Delta^2-\omega^2}}$. In such subgap regime, the single-particle spectral function $\rho_d(\omega) \equiv -\frac{1}{\pi}\mathrm{Im}\left\{\boldsymbol{G}_{d,11}(\omega)\right\}$ has the BCS structure

$$\rho_d(\omega) = \frac{1}{2\pi}\left[1+\frac{\varepsilon_d}{\tilde{E}_d}\right]\frac{\Gamma_N/2}{(\tilde{\omega}-\tilde{E}_d)^2+(\Gamma_N/2)^2} + \frac{1}{2\pi}\left[1-\frac{\varepsilon_d}{\tilde{E}_d}\right]\frac{\Gamma_N/2}{(\tilde{\omega}+\tilde{E}_d)^2+(\Gamma_N/2)^2} \tag{8}$$

with ω-dependent $\tilde{E}_d = \sqrt{\varepsilon_d^2 + \left(\tilde{\Gamma}_s/2\right)^2}$. Figure 1 shows the spectrum $\rho_d(\omega)$ of the uncorrelated quantum impurity obtained for the energy level $\varepsilon_d = -\Gamma_S/2$ in limit of weak coupling $\Gamma_N = 0.0005\Gamma_S$. Depending on the ratio Δ/Γ_S we can notice the appearance of the in-gap states whose position gradually evolves from the gap edge singularities (when $\Delta \ll \Gamma_S$) to $\pm\sqrt{\varepsilon_d^2 + \Gamma_S^2/4}$ (when $\Delta \gg \Gamma_S$). These in-gap features are known in the literature as the Shiba [13] or Andreev states. Let us remark that these Shiba states appear simultaneously at negative and positive energies, because of the particle-hole mixing characteristic for the electron pairing.

For an infinitesimally small coupling Γ_N, the in-gap states have a resonant character (see Figure 2). In other words, the in-gap Shiba states represent the infinite life-time quasiparticles for $\Gamma_N \to 0^+$. In the subgap regime, the spectral function (8) has two quasiparticle peaks at energies $\omega = E_\pm$, which formally represent the poles of the single-particle Green's function $\boldsymbol{G}_d(\omega)$. For the uncorrelated quantum impurity, they simplify the solution of the following equation [34]

$$E_\pm + \frac{\Gamma_S}{2}\frac{E_\pm}{\sqrt{\Delta^2 - E_\pm^2}} = \pm\sqrt{\varepsilon_d^2 + \left(\frac{\Gamma_S}{2}\right)^2 \frac{\Delta^2}{\Delta^2 - E_\pm^2}}. \tag{9}$$

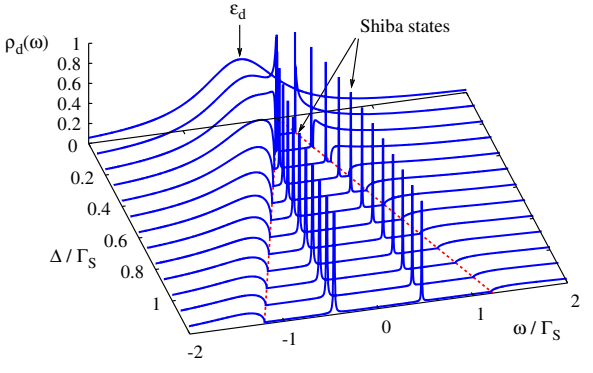

Figure 1. (colour online) Spectrum $\rho_d(\omega)$ of the uncorrelated quantum dot obtained for $\varepsilon_d/\Gamma_S = -0.5$ assuming a weak coupling to the metallic lead $\Gamma_N = 0.0005\Gamma_S$. The subgap (Shiba or Andreev) features gradually emerge from the gap edge singularities $\pm\Delta$ (dashed lines) and evolve into well developed in-gap quasiparticles for $\Delta \gg \Gamma_S$.

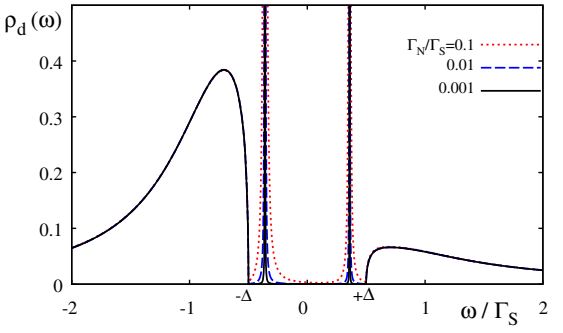

Figure 2. (colour online) Energy spectrum $\rho_d(\omega)$ of the uncorrelated quantum dot obtained for $\varepsilon_d/\Gamma_S = -0.5$, $\Delta/\Gamma_S = 0.5$ and several couplings to the metallic lead $\Gamma_N/\Gamma_S = 0.001$, 0.01 and 0.1 (as indicated).

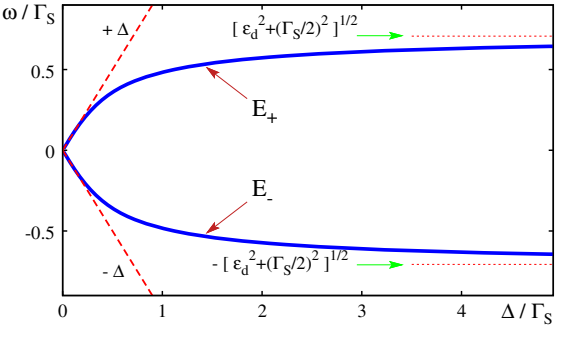

Figure 3. (colour online) Energies $E_\pm$ of the Shiba quasiparticles of the uncorrelated quantum impurity ($U = 0$) obtained for $\varepsilon_d = -0.5\Gamma_S$ assuming the infinitesimally small coupling Γ_N. Notice, that for $\Delta \gg \Gamma_S$ they asymptotically tend to $E_\pm = \pm\sqrt{\varepsilon_d^2 + (\Gamma_S/2)^2}$.

In Figure 3, we plot the energies $E_\pm$ as a function of the ratio Δ/Γ_S for $\varepsilon_d = -0.5\Gamma_S$. In the limit $\Delta \ll \Gamma_S$ these resonant in-gap states are located nearby the gap edge singularities $\pm\Delta$ [18]. For larger values of the ratio Δ/Γ_S, they move away from the gap edge singularities and asymptotically approach the values $\pm\sqrt{\varepsilon_d + (\Gamma_S/2)^2}$ in the limit $\Delta \gg \Gamma_S$. In the next Sections 5 and 6, we shall consider the correlation effects for such 'superconducting atomic limit' $\Delta \gg \Gamma_S$.

5. Spin-exchange interactions

In the limit of strong coupling to superconducting electrode, the selfenergy $\Sigma_0(\omega)$ simplifies to a static value and the superconducting electrode is then responsible for the induced on-dot pairing gap $\Delta_d = \Gamma_S/2$. We shall now address the correlation effects using the following auxiliary Hamiltonian

$$\hat{H} = \sum_{\sigma} \epsilon_d \hat{d}^{\dagger}_{\sigma} \hat{d}_{\sigma} + U_d \, \hat{n}_{d\uparrow} \hat{n}_{d\downarrow} - \Delta_d \left(\hat{d}^{\dagger}_{\uparrow} \hat{d}^{\dagger}_{\downarrow} + \hat{d}_{\downarrow} \hat{d}_{\uparrow} \right) + \hat{H}_N + \sum_{\mathbf{k},\sigma} \left(V_{\mathbf{k}N} \, \hat{d}^{\dagger}_{\sigma} \hat{c}_{\mathbf{k}\sigma N} + \text{h.c.} \right). \tag{10}$$

In particular, we would like to determine interplay between the induced on-dot pairing gap Δ_d and the many body Kondo-type correlations, which arise from a combined effect of the hybridization $V_{\mathbf{k}N}$ and the Coulomb repulsion U_d.

For the case $\Delta_d = 0$, the effective spin-exchange interaction (between impurity and itinerant electrons) has been inferred from the famous Schrieffer–Wolf transformation [35]. Treating the hybridization term $\sum_{\mathbf{k}\sigma} \left(V_{\mathbf{k},N} \hat{c}^{\dagger}_{\mathbf{k}\sigma N} \hat{d}_{\sigma} + V^{*}_{\mathbf{k},N} \hat{d}^{\dagger}_{\sigma} \hat{c}_{\mathbf{k}\sigma N} \right)$ as a small perturbation the authors constructed the unitary transformation $e^{\hat{S}} \hat{H} e^{-\hat{S}}$. Using the antihermitean operator

$$\hat{S} = \sum_{\mathbf{k},\sigma} V_{\mathbf{k},N} \left(\frac{\hat{c}^{\dagger}_{\mathbf{k}\sigma N} \hat{d}_{\sigma}}{\xi_{\mathbf{k}N} - \varepsilon_d} + \frac{U \, \hat{c}^{\dagger}_{\mathbf{k}\sigma N} \hat{d}_{\sigma} \hat{n}_{d,-\sigma}}{(\varepsilon_d - \xi_{\mathbf{k}N})(\varepsilon_d + U_d - \xi_{\mathbf{k}N})} \right) - \text{h.c.} \tag{11}$$

they have derived the Kondo-type Hamiltonian with the induced exchange interaction $\hat{H}_{\text{exch}} = -\sum_{\mathbf{k},\mathbf{p}} J_{\mathbf{kp}} \hat{\mathbf{s}}_d \cdot \hat{\mathbf{S}}_{\mathbf{kp}}$ between the impurity spin $\hat{\mathbf{s}}_d$ and the spins $\hat{\mathbf{S}}_{\mathbf{kp}}$ of itinerant electrons. Near the Fermi surface the exchange coupling turned out to be antiferromagnetic (negative) and its magnitude has been estimated as $J_{\mathbf{k}_F\mathbf{p}_F} = -4|V_{\mathbf{k}_F N}|^2/U_d$. This antiferromagnetic interaction is at low temperatures responsible for a narrow Abrikosov-Suhl resonance appearing in the quantum dot spectrum at $\omega \sim \mu_N$.

The Schrieffer–Wolf transformation has been later re-examined in a more systematic way by Kehrein and Mielke [36] going beyond the perturbative scheme. Their study was based on the continuous unitary transformation $\hat{\mathcal{U}}(l) \hat{H} \hat{\mathcal{U}}^{\dagger}(l)$ eliminating the hybridization term via a sequence of the infinitesimal transformations, upon varying the *flow* parameter l. In the present study, we generalize their treatment to the model Hamiltonian (10) with the induced on-dot pairing Δ_d.

We design the continuous unitary transformation $\mathcal{U}(l)$ following the original framework introduced by Wegner [37], who proved that the generating generator $\hat{\eta}(l) \equiv \frac{\partial \hat{\mathcal{U}}(l)}{\partial l} \hat{\mathcal{U}}^{-1}(l)$ chosen in the form $\hat{\eta}(l) = \left[\hat{H}_0(l), \hat{V}(l) \right]$ enforces $\hat{V}(l)$ to vanish in the limit $l \to \infty$. Applying this method to the Hamiltonian (10), we find the antihermitean operator $\hat{\eta}(l) = \hat{\eta}_0(l) - \hat{\eta}^{\dagger}_0(l)$, where

$$\hat{\eta}_0(l) = \sum_{\mathbf{k}\sigma} \left(\eta_{\mathbf{k}}(l) + \eta^{(2)}_{\mathbf{k}}(l) \hat{n}_{d,-\sigma} \right) \hat{c}^{\dagger}_{\mathbf{k}\sigma N} \hat{d}_{\sigma} + \sum_{\mathbf{kp}\sigma} \eta_{\mathbf{kp}}(l) \hat{c}^{\dagger}_{\mathbf{k}\sigma N} \hat{c}_{\mathbf{p}\sigma N} + \sum_{\mathbf{k}} \eta^{(1)}_{\mathbf{k}}(l) \left(\hat{c}^{\dagger}_{\mathbf{k}\uparrow N} \hat{d}^{\dagger}_{\downarrow} - \hat{c}^{\dagger}_{\mathbf{k}\downarrow N} \hat{d}^{\dagger}_{\uparrow} \right) \tag{12}$$

with the l-dependent amplitudes $\eta_{\mathbf{k}}(l) = (\xi_{\mathbf{k}}(l) - \varepsilon_{\mathbf{d}}(l)) V_{\mathbf{k}}(l)$, $\eta_{\mathbf{kp}}(l) = V_{\mathbf{k}}(l) V_{\mathbf{p}}(\mathrm{l})$, $\eta^{(1)}_{\mathbf{k}}(l) = \Delta_{\mathbf{d}}(l) V_{\mathbf{k}}(l)$ and $\eta^{(2)}_{\mathbf{k}}(l) = -U_d(l) V_{\mathbf{k}}(l)$. The continuous unitary transformation $\hat{\mathcal{U}}(l) \hat{H} \hat{\mathcal{U}}^{\dagger}(l)$ affects all parameters of the Hamiltonian (10) changing them into l-dependent quantities $\varepsilon_d(l)$, $u_d(l)$, $\Delta_d(l)$ and $V_{\mathbf{k}N}(l)$. They are renormalized through the flow equation of the l-dependent Hamiltonian [37]

$$\frac{\partial \hat{H}(l)}{\partial l} = [\hat{\eta}(l), \hat{H}(l)]. \tag{13}$$

During such l-dependent evolution, there appear also additional terms, e.g. the spin–spin interaction $-\sum_{\mathbf{k},\mathbf{p}} J_{\mathbf{kp}}(l)\hat{\mathbf{s}}_d \cdot \hat{\mathbf{S}}_{\mathbf{kp}}$ with the boundary condition $J_{\mathbf{kp}}(l=0)=0$. Neglecting other less relevant processes (like the pair hopping, density-density interaction and pairing between the quantum dot and metallic lead), we obtain the following set of coupled *flow equations*

$$\frac{\partial \varepsilon_d(l)}{\partial l} = -2\sum_{\mathbf{k}} \eta_{\mathbf{k}}(l) V_{\mathbf{k}N}(l), \tag{14}$$

$$\frac{\partial U_d(l)}{\partial l} = -4\sum_{\mathbf{k}} \eta^{(2)}_{\mathbf{k}}(l) V_{\mathbf{k}N}(l), \tag{15}$$

$$\frac{\partial \Delta_d(l)}{\partial l} = 2\sum_{\mathbf{k}} \eta^{(1)}_{\mathbf{k}}(l) V_{\mathbf{k}N}(l), \tag{16}$$

$$\begin{aligned}\frac{\partial V_{\mathbf{k}}(l)}{\partial l} &= \eta_{\mathbf{k}}(l)\left[\varepsilon_d(l) - \xi_{\mathbf{k}N} + U_d(l)\langle \hat{n}_{d,\sigma}\rangle\right] + \sum_{\mathbf{p}} \eta_{\mathbf{kp}}(l) V_{\mathbf{p}N}(l) \\ &\quad -\eta^{(1)}_{\mathbf{k}}(l)\Delta_d(l) + \eta^{(2)}_{\mathbf{k}}(l)\left[\varepsilon_d(l) - \xi_{\mathbf{k}N} + U_d(l)\right]\langle \hat{n}_{d,\sigma}\rangle\end{aligned} \tag{17}$$

$$\frac{\partial J_{\mathbf{kp}}(l)}{\partial l} = \eta^{(2)}_{\mathbf{k}}(l) V_{\mathbf{p}N}(l) + \eta^{(2)}_{\mathbf{p}}(l) V_{\mathbf{k}N}(l) - (\xi_{\mathbf{k}N} - \xi_{\mathbf{p}N})^2 J_{\mathbf{kp}}(l). \tag{18}$$

In the present study, we explore these equations, focusing on the half-filled quantum dot $n_{d\sigma} = 0.5$, $\varepsilon_d = -U_d/2$ (a more complete analysis shall be discussed elsewhere).

To derive the lowest order estimations, we can solve the flow Equations (14)–(18) assuming the weak hybridization $V_{\mathbf{k}N}$. Since the unitary transformation is then expected to affect mainly the coupling strength $V_{\mathbf{k}N}(l)$ we can omit l-dependence of all other parameters in the Equation (17). Such (approximate) treatment implies an exponential scaling

$$V_{\mathbf{k}N}(l) = V_{\mathbf{k}N}\, \exp\left[-f_{\mathbf{k}} l\right], \tag{19}$$

where $f_{\mathbf{k}} = (\varepsilon_d - \xi_{\mathbf{k}N})^2 + \Delta_d^2 - \xi_{\mathbf{k}N} U_d$. We thus see that the hybridization coupling (19) vanishes in the asymptotic limit $l \to \infty$.

Substituting (19) on the right hand side of the flow Equations (14)–(16) and (18) we can in turn estimate the other l-dependent quantities. In particular, the exchange coupling is renormalized according to

$$J_{\mathbf{kp}}(l) = \frac{-2U V_{\mathbf{k}N} V_{\mathbf{p}N}}{f_{\mathbf{k}} + f_{\mathbf{p}} - \left(\xi_{\mathbf{k}N} - \xi_{\mathbf{p}N}\right)^2}\left[1 - e^{-(f_{\mathbf{k}} + f_{\mathbf{p}})l}\right]. \tag{20}$$

It approaches asymptotically the following effective value

$$J_{\mathbf{kp}}(\infty) = \frac{-2U V_{\mathbf{k}N} V_{\mathbf{p}N}}{(\varepsilon_d - \xi_{\mathbf{k}N})^2 + \left(\varepsilon_d - \xi_{\mathbf{p}N}\right)^2 + \Delta_d^2 - \left(\xi_{\mathbf{k}N} + \xi_{\mathbf{p}N}\right) U_d - \left(\xi_{\mathbf{k}N} - \xi_{\mathbf{p}N}\right)^2}$$

and (for $\varepsilon_d = -U_d/2$) near the Fermi surface has an antiferromagnetic character

$$J_{\mathbf{k}_F\mathbf{p}_F}(l \to \infty) = \frac{-4U_d |V_{\mathbf{k}_F N}|^2}{U_d^2 + (2\Delta_d)^2}. \tag{21}$$

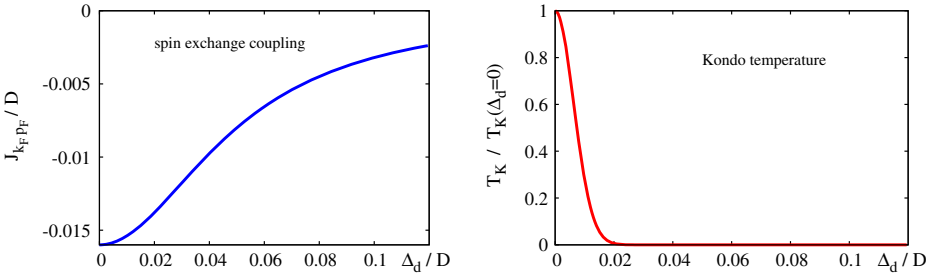

Figure 4. (colour online) Variation of the effective antiferromagnetic exchange coupling $J_{\mathbf{k}_F\mathbf{p}_F}$ (left h.s. panel) and the Kondo temperature (right h.s. panel) with respect to the induced on-dot energy gap Δ_d. The results are obtained for the symmetric quantum impurity model ($\varepsilon_d = -U/2$) assuming the weak coupling $V_{\mathbf{k}}/D = 0.02$ and the Coulomb potential $U/D = 0.1$.

Comparing (21) to the Schrieffer–Wolf formula $J_{\mathbf{k}_F\mathbf{p}_F} = -4|V_{\mathbf{k}_F N}|^2/U_d$ [35] we notice that the induced on-dot gap Δ_d substantially weakens the antiferromagnetic coupling. From a physical point of view, this detrimental influence originates from the competition between magnetism and superconductivity. We illustrate this influence in Figure 4. Since Δ_d is controlled by the hybridization Γ_S (which can be varied experimentally) such interplay between the pairing and the spin correlations can be explored in a tunable way. To estimate the Kondo temperature T_K, we make use of the Bethe-ansatz relationship [38]

$$T_K = \frac{2D}{\pi k_B} \exp\left\{-\phi\left[2\rho(\varepsilon_{\mathbf{F}}) J_{\mathbf{k}_F\mathbf{p}_F}(\infty)\right]\right\}, \tag{22}$$

where k_B is the Boltzmann's constant, $\rho(\varepsilon_F)$ denotes the density of states at the Fermi level and $\phi(y) \simeq |y|^{-1} - 0.5\ln|y|$. The right-hand side panel in Figure 4 shows the Kondo temperature obtained from (22) as a function of the induced pairing gap Δ_d. This result (21) qualitatively agrees with the recent experimental data [2].

6. Spectroscopic signatures of the subgap Kondo effect

To support the results obtained in the previous section concerning detrimental influence of the proximity induced pairing on the Kondo-type correlations, we analyse here the subgap spectrum using another (complementary) method. In order to determine the matrix selfenergy

$$\mathbf{\Sigma}_d^0(\omega) + \mathbf{\Sigma}_d^U(\omega) \equiv \begin{pmatrix} \Sigma_{11}(\omega) & \Sigma_{12}(\omega) \\ [\Sigma_{12}(-\omega)]^* & -[\Sigma_{11}(-\omega)]^* \end{pmatrix} \tag{23}$$

we adopt some approximations for treating the Coulomb repulsion $U_d\hat{n}_{d\uparrow}\hat{n}_{d\downarrow}$. In what follows, we analyse their influence by a decoupling scheme imposed onto the lowest order Green's functions.

As a first step, we express the diagonal part of $\boldsymbol{G}_d$ by the BCS-type formula [39]

$$[\boldsymbol{G}_{11}(\omega)]^{-1} = \omega - \varepsilon_d - \Sigma_{11}(\omega) - \frac{\Delta_d^2}{\omega + \varepsilon_d + [\Sigma_{11}(-\omega)]^*}, \tag{24}$$

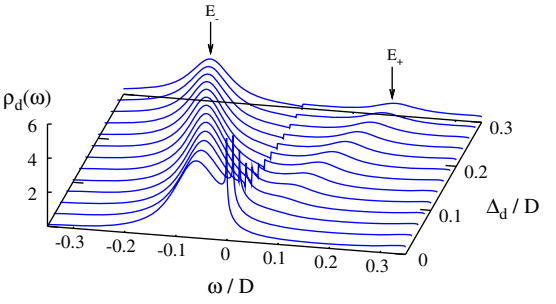

Figure 5. (colour online) Low-energy spectrum of the correlated quantum dot obtained for $\varepsilon_d/D = -0.075$, $V_{\mathbf{k}}/D = 0.1$ in the strong interaction limit $U_d \gg \Gamma_S$ and assuming $\Delta \gg \Gamma_S$. We can notice that the Kondo peak (at $\omega = 0$) is suppressed upon increasing the induced on-dot pairing Δ_d and simultaneously the subgap states $E_\pm = \pm\sqrt{\varepsilon_d^2 + \Delta_d^2}$ are pushed away.

where $\Sigma_{11}(\omega)$ is taken from the popular Meir and Wingreen estimation [40]

$$\Sigma_{11}(\omega) \simeq U_d\left[n_{d,\bar{\sigma}} - \Sigma_1(\omega)\right] + \frac{U_d\left[n_{d,\sigma} - \Sigma_1(\omega)\right]\left[\Sigma_3(\omega) + U_d(1-n_{d,\sigma})\right]}{\omega - \varepsilon_d - \Sigma_0(\omega) - \left[\Sigma_3(\omega) + U_d(1-n_{d,\bar{\sigma}})\right]}. \quad (25)$$

In expression (25), we recognize the usual non-interacting contribution $\Sigma_0(\omega) = -i\Gamma_N/2$ and two additional terms

$$\Sigma_\nu(\omega) = \sum_{\mathbf{k}} |V_{\mathbf{k}N}|^2 \left[\frac{1}{\omega - \xi_{\mathbf{k}N}} + \frac{1}{\omega - U_d - 2\varepsilon_d + \xi_{\mathbf{k}N}}\right] \times \begin{cases} f(\xi_{\mathbf{k}N}) & \text{for } \nu = 1 \\ 1 & \text{for } \nu = 3 \end{cases} \quad (26)$$

which are responsible for the Coulomb blockade ($\nu = 3$) and the Kondo effect ($\nu = 1$). The off-diagonal Green's function $\boldsymbol{G}_{12}(\omega)$ indirectly depends on $\boldsymbol{G}_{11}(\omega)$ via the (exact) relation

$$(\omega - \varepsilon_d)\,\boldsymbol{G}_{11}(\omega) = 1 + U_d \langle\langle \hat{d}_\uparrow \hat{n}_{d\downarrow}; \hat{d}_\uparrow^\dagger \rangle\rangle(\omega) - \Delta_d \boldsymbol{G}_{12}(\omega). \quad (27)$$

Since the proximity induced pairing Δ_d should have a rather marginal influence on the two-particle propagator $\langle\langle \hat{d}_\uparrow \hat{n}_{d\downarrow}; \hat{d}_\uparrow^\dagger \rangle\rangle(\omega)$ we follow [40] using the approximation

$$\langle\langle \hat{d}_\uparrow \hat{n}_{d\downarrow}; \hat{d}_\uparrow^\dagger \rangle\rangle(\omega) \simeq \frac{n_{d\downarrow} - \Sigma_1(\omega)\ \boldsymbol{G}_{11}(\omega)}{\omega - \varepsilon_d - \Sigma_0(\omega) - U_d - \Sigma_3(\omega)}. \quad (28)$$

In this way, we complete the first guess for the matrix Green's function $\boldsymbol{G}_d(\omega)$. Next, we update iteratively the initial Ansatz (24) using the following identity

$$[\boldsymbol{G}_{11}(\omega)]^{-1} = \omega - \varepsilon_d - \Sigma_{11}(\omega) - \frac{\boldsymbol{\Sigma}_{12}(\omega)\,[\boldsymbol{\Sigma}_{12}(-\omega)]^*}{\omega + \varepsilon_d + [\Sigma_{11}(-\omega)]^*}. \quad (29)$$

Within this scheme, we have numerically calculated the Green's function $\boldsymbol{G}_d(\omega)$ for the energy band D discretized into 10^3 equidistant points. We obtained a fairly satisfactory convergence already after 10 iterations. Figure 5 shows an evolution of the spectral function $\rho_d(\omega)$ for varying Δ_d. For clarity, we focus on the low-energy regime, where both the pairing and Kondo effects are strongly manifested. In the high-energy regime, we could additionally observe the Coulomb satellite peak near $\omega \sim \varepsilon_d + U_d$ and a continuous background outside the superconductor gap $|\omega| \geq \Delta$.

For $\Delta_d = 0$, the diverging real part of $\Sigma_1(\omega)$ induces the narrow Kondo peak at μ_N [40] (we use here μ_N as the reference level for energies). The increasing Δ_d leads to the following qualitative changes: (i) splitting of the initial Lorentzian at ε_d into the lower E_- and upper E_+ quasiparticle peaks, and (ii) gradual suppression of the Kondo resonance. The particle-hole splitting originates solely from the induced on-dot pairing (as has been discussed in Section 4), whereas the zero-energy resonance is due to the spin singlet driven by the exchange interactions. We thus interpret the behaviour shown in Figure 5 as a signature of a destructive influence of the on-dot pairing on the Kondo-type correlations in analogy to what has been predicted for the Josephson junctions [41]. In the present context (for the metal-quantum-dot–superconductor junctions), the experimental measurements do indeed indicate such tendency [1,2].

7. Conclusions

We have studied the spectroscopic signatures of the proximity induced electron pairing in the metal-quantum-dot–superconductor heterojunction. Excitation spectrum of the quantum dot is characterized by the particle and hole peaks (so called, the Andreev or Shiba states) formed in a subgap region $|\omega| < \Delta$. Their broadening (i.e. inverse life-time) is controlled by a hybridization Γ_N to the metallic electrode, whereas the induced pairing gap Δ_d predominantly depends on a hybridization Γ_S with the superconducting electrode.

We have addressed an interplay between such induced on-dot paring and the electron correlations due to strong Coulomb repulsion. Using two complementary methods of: (a) the continuous unitary transformation and (b) the self-consistent iterative scheme for the decoupled Green's functions we have analysed the influence of the induced on-dot pairing on the Kondo-type correlations. Both methods clearly show that the on-dot pairing has a detrimental influence on the Kondo effect. As a consequence of their competition, the quantum dot spectrum does either reveal the narrow Kondo resonance (when $\Gamma_N < \Gamma_S$) or the separated particle and hole Shiba peaks (when $\Gamma_S \gg \Gamma_N$). In a coexistence region $\Gamma_N \sim \Gamma_S$, the Kondo resonance does eventually show up in the subgap (Andreev) conductance as has been evidenced experimentally [1,2,42].

Nanoscopic heterostructures comprising the correlated quantum dots coupled to the external metallic, superconducting and/or ferromagnetic electron reservoirs can be thus a valuable testing ground for exploring the many-body effects in a tunable way. In particular, one can investigate relationship between the induced electron pairing and the Coulomb repulsion accessing even the Kondo regime [17,27,43–45]. Such possibility is much more difficult to realize in the solid-state physics [10].

Acknowledgements

We acknowledge discussions with Johannes Bauer and Karol I. Wysokiński.

References

[1] R.S. Deacon, Y. Tanaka, A. Oiwa, R. Sakano, K. Yoshida, K. Shibata, K. Hirakawa and S. Tarucha, Phys. Rev. Lett. 104 (2010) p.076805; R.S. Deacon, Y. Tanaka, A. Oiwa, R. Sakano, K. Yoshida, K. Shibata, K. Hirakawa and S. Tarucha, Phys. Rev. B 81 (2010) p.121308(R).

[2] E.J.H. Lee, X. Jiang, R. Aguado, G. Katsaros, C.M. Lieber and S. De Franceschi, Phys. Rev. Lett. 109 (2012) p.186802.

[3] E.J.H. Lee, X. Jiang, M. Houzet, R. Aguado, ChM Lieber and S. De Franceschi, Nat. Nanotechnol. 9 (2014) p.79.

[4] J.D. Pillet, P. Joyez, R. Žitko and F.M. Goffman, Phys. Rev. B 88 (2013) p.045101.

[5] E.J.H. Lee, X. Jiang, J. Schindele, A. Baumgartner, R. Maurand, M. Weiss and C. Schönenberger, Phys. Rev. B 89 (2014) p.045422.

[6] J.-D. Pillet, C.H.L. Quay, P. Morfin, C. Bena, A. Levy-Yeyati and P. Joyez, Nature Phys. 6 (2010) p.965.

[7] T. Dirks, T.L. Hughes, S. Lal, B. Uchoa, Y.-F. Chen, C. Chialvo, P.M. Golbart and N. Mason, Nature Phys. 7 (2011) p.386.

[8] L. Bretheau, C.Ö. Girit, H. Pothier, D. Esteve and C. Urbina, Nature 499 (2013) p.312.

[9] H.I. Jogensen, T. Novotný, K. Grove-Rasmussen, K. Flensberg and P.E. Lindelof, Phys. Rev. Lett. 104 (2010) p.076805; V. Janiš, V. Pokorný and M. Žonda, Nano Lett. 7 (2007) p.2441.

[10] A.V. Balatsky, I. Vekhter and J.-X. Zhu, Rev. Mod. Phys. 78 (2006) p.373.

[11] P.W. Anderson, J. Phys. Chem. Solids 11 (1959) p.26.

[12] A.A. Abrikosov and L.P. Gorkov, Sov. Phys. JETP 12 (1961) p.1243.

[13] Yu. Luh, Acta Phys. Sin. 21 (1965) p.75; H. Shiba, Prog. Theor. Phys. 40 (1968) p.435; A.I. Rusinov, Sov. Phys. JETP 56 (1969) p.2047; H. Shiba and T. Soda, Prog. Theor. Phys. 41(1969) p.25.

[14] A.C. Hewson, *The Kondo Problem to Heavy Fermions*, Cambridge University Press, Cambridge, 1993.

[15] A. Martín-Rodero and A. Levy-Yeyati, Adv. Phys. 60 (2011) p.899.

[16] S. De Franceschi, L. Kouwenhoven, C. Schönenberger and W. Wernsdorfer, Nat. Nanotechnol. 5 (2010) p.703.

[17] R. Maurand and Ch. Schönenberger, Physics 6 (2013) p.75; J.D. Pillet, P. Joyez, R.Žitko, F.M. Goffman, Phys. Rev. B 88 (2013) p.045101.

[18] J. Bauer, A. Oguri and A.C. Hewson, J. Phys.: Condens. Matter 19 (2008) p.486211.

[19] R. Fazio and R. Raimondi, Phys. Rev. Lett. 80 (1998) p.2913; Phys. Rev. Lett. 82 (1999) p.4950.

[20] P. Schwab and R. Raimondi, Phys. Rev. B 59 (1999) p.1637.

[21] M. Krawiec and K.I. Wysokiński, Supercond. Sci. Technol. 17 (2004) p.103.

[22] A.A. Clerk, V. Ambegaokar and S. Hershfield, Phys. Rev. B 61 (2000) p.3555.

[23] J.C. Cuevas, A. Levy Yeyati and A. Martin-Rodero, Phys. Rev. B 63 (2001) p.094515.

[24] Y. Yamada, Y. Tanaka and N. Kawakami, Phys. Rev. B 84 (2011) p.075484.

[25] Y. Avishai, A. Golub and A.D. Zaikin, Phys. Rev. B 63 (2001) p.134515; Y. Avishai, A. Golub and A.D. Zaikin, Phys. Rev. B 68 (2003) p.045312.

[26] Y. Tanaka, N. Kawakami and A. Oguri, J. Phys. Soc. Jpn. 76 (2007) p.074701; Y. Tanaka and N. Kawakami, Phys. Rev. B 84 (2011) p.075484.

[27] A. Oguri, Y. Tanaka and J. Bauer, Phys. Rev. B 87 (2013) p.075432.

[28] T. Domański and A. Donabidowicz, Phys. Rev. B 76 (2008) p.073105; T. Domański, A. Donabidowicz and K.I. Wysokiński, Phys. Rev. B 76 (2007) p.104514.

[29] C. Karrasch, A. Oguri and V. Meden, Phys. Rev. B 77 (2008) p.024517; C. Karrasch and V. Meden, Phys. Rev. B 79 (2009) p.045110.

[30] V. Koerting, B.M. Andersen, K. Flensberg and J. Paaske, Phys. Rev. B 82 (2010) p.245108; B.M. Andersen, K. Flensberg. V. Koerting and J. Paaske, Phys. Rev. Lett. 107 (2011) p.256802.

[31] A. Koga, Phys. Rev. B 87 (2013) p.115409.

[32] K. Kang, Phys. Rev. B 58 (1998) p.9641; S.Y. Cho, K. Kang and C.-M. Ryu, Phys. Rev. B 60 (1999) p.16874.

[33] Q.-F. Sun, J. Wang and T.-H. Lin, Phys. Rev. B 59 (1999) p.3831; Q.-F. Sun, H. Guo and T.-H. Lin, Phys. Rev. Lett. 87 (2001) p.176601.

[34] J. Barański and T. Domański, J. Phys.: Condens. Matter 25 (2013) p.435305.

[35] J.R. Schrieffer and P.A. Wolff, Phys. Rev. 149 (1966) p.491.
[36] S. Kehrein and A. Mielke, J. Phys. A: Math. Gen. 27 (1994) p.4259; S. Kehrein and A. Mielke, Ann. Phys. 252 (1996) p.1.
[37] F. Wegner, Ann. Physik (Leipzig) 3 (1994) p.77.
[38] A.M. Tsvelick and P.B. Wiegmann, Adv. Phys. 32 (1983) p.453.
[39] K. Levin, Q. Chen, C.-C. Chien and Y. He, Annals of Physics 325, 233 (2010); T. Domański and J. Ranninger: Phys. Rev. Lett. 91 (2003) p.255301.
[40] Y. Meir, N.S. Wingreen and P.A. Lee, Phys. Rev. Lett. 66 (1991) p.3048.
[41] L.I. Glazman and K.A. Matveev, Zh. Eksp. Teor. Fiz. Pis'ma Red. 49 (1989) p.570. [JETP Lett. 49, 659 (1989)].
[42] W. Chang, V.E. Manucharyan, T.S. Jaspersen, J. Nygård and C.M. Marcus, Phys. Rev. Lett. 110 (2013) p.217005.
[43] D. Futturrer, J. Swiebodzinski, M. Governale and J. König, Phys. Rev. B 87 (2013) p.014509; D. Futturrer, M. Governale and J. König, EPL 91 (2010) p.47004.
[44] A. Cottet, T. Kontos and A. Levy, Yeyati: Phys. Rev. Lett. 108 (2012) p.166803.
[45] S. Droste, S. Andergassen and J. Splettstoesser, J. Phys.: Condens. Matter 24 (2012) p.415301; S. Grap, V. Meden and S. Andergassen, Phys. Rev. B 86 (2012) p.035143.